

A potential framework for cross-zonal reserve procurement on European power exchanges based on robust optimization

Dániel Divényi^a, Ádám Sleisz^{a,*}, Péter Sórés^a, Dávid Csercsik^{b,c}, Bálint Hartmann^a

^a Department of Electric Power Engineering, Budapest University of Technology and Economics, Egy József u. 18., 1111 Budapest, Hungary

^b Institute of Economics, Centre for Economic and Regional Studies, Tóth Kálmán u. 4., 1097 Budapest, Hungary

^c Faculty of Information Technology and Bionics, Pázmány Péter Catholic University, Práter u. 50/A., 1083 Budapest, Hungary

ARTICLE INFO

Keywords:

Power exchange
Ancillary services
Network modeling
Robust optimization
Internal Energy Market

ABSTRACT

In order to prepare for unexpected events in the power system, regulation reserves are routinely procured in advance. Economic considerations dictate that it is advantageous to perform reserve procurement and energy allocation on a joint market platform using a single clearing algorithm. Furthermore, it is also beneficial if the option exists to allocate resources between different bidding zones to alleviate local shortages and corresponding price pressures. The present paper proposes a solution algorithm for this task in a European market environment without unit commitment and uplift payments to non-convex bidders. The main challenge of cross-zonal reserve allocation arises from the fact that deployment decisions are not yet known, therefore the actual deployment flows are uncertain at the time of procurement. The proposed algorithm handles this issue with robust optimization techniques and provides a guarantee of feasible transmission limits for deployment i.e. reserve deliverability. The clearing model is formalized as a computationally efficient Mixed Integer Linear Problem; its exact equations are presented along with case studies for the purpose of demonstration. The research is part of the FARCROSS H2020 project of the European Union.

1. Introduction

The imbalance of electricity generation and consumption is a recurring phenomenon in the power system. Its appearance is usually linked to uncertain events such as network faults. Although intraday energy markets are able to handle some of the energy imbalance, their liquidity is not always sufficient. Consequently, the procurement of load-frequency regulation reserves with specific technical requirements (e.g. activation in a closed-loop control) is a traditional and common method to prepare for imbalance contingencies in the power system [1]. The capability to control a certain portion of power generation or consumption is necessary to stabilize system frequency through reliable power balance. This need of flexibility is exacerbated in Europe by the increasing market share of weather-dependent renewable generation that aims to reduce carbon emissions [2]. Furthermore, the task of flexibility service supply often falls on gas-fired power plants due to their relative advantages in efficiency, generation gradient dynamics and cleanliness [3] but the European price of natural gas is subject to difficult trade relations and outright manipulation [4]. Considering these challenges, it is vitally important to find market designs that allow

the most efficient allocation of reserves.

The markets of energy and reserves are closely interdependent because they utilize the same generation and consumption capabilities of market actors and the same transfer capacity of the grid. One of the consequences of this interdependence is that the simultaneous and joint trading of energy and reserves is considered to be beneficial from the economic viewpoint [5]. Furthermore, the advantages of co-allocation are expected to grow with the increasing share of renewable generation [6]. The construction of a joint trading platform is a potential next step of European market integration. The FARCROSS H2020 project [7] of the European Union has elaborated several aspects of this aspiration. This paper presents some of the relevant results.

The connection between energy and reserves is so close that reserves can be considered as option products of energy [8]. Procurement requires the service provider to withhold or release its controllable power for a fixed period of time i.e. to withhold or release energy. For the sake of simplicity, reserve bids and allocations are described in this paper using their underlying energy quantity instead of power values. We assume hourly reserve procurement, therefore a reserve bid of 30 MW power appears with its 30 MWh underlying energy.

* Corresponding author.

E-mail address: sleisz.adam@bme.hu (Á. Sleisz).

<https://doi.org/10.1016/j.segan.2023.101267>

Received 17 July 2023; Received in revised form 2 November 2023; Accepted 28 December 2023

Available online 30 December 2023

2352-4677/© 2023 The Authors. Published by Elsevier Ltd. This is an open access article under the CC BY-NC-ND license (<http://creativecommons.org/licenses/by-nc-nd/4.0/>).

One of the hardest challenges in the research area of energy-reserve co-allocation is about the effect of network transmission limits on reserve services. The procurement of reserves in itself does not imply any physical, firm power flow on the grid, therefore it is not directly constrained by network bottlenecks. However, the transmission limits of the grid are binding indirectly because procured reserves are deployed (or synonymously: activated) later when imbalances actually happen, and they should be deliverable. In the case of activation, physical power flow does happen and network constraints apply accordingly. The main issue is that it is generally unknown at the time of procurement where and when activated reserves will be delivered (or if they will be activated at all). Due to this uncertainty, the management of potential network congestions resulting from possible deployment is not as straightforward as the widely used modeling of transmission limits for energy-only, scheduled product cross-zonal exchanges.

Fig. 1 illustrates the most important differences between the allocation of energy and reserve products for a single transmission line using a zonal network model. The line is assumed to run between bidding zones A and B; it has 120 MWh hourly capacity in both directions. The expected energy flow arising from the energy allocation is denoted by a black bar while the capacity allocation for upward reserve is shown in red. In the middle, 60 MWh of energy is allocated from A to B and 20 MWh energy from B to A. These exchanged quantities are firm deliveries, thus netting in this implicit allocation of transmission rights is possible. The eventual result is an hourly flow of 40 MWh from A to B. On the right, the allocation dictates to withhold the same amount of energy as upward control reserve with the potential activation of 60 MWh from A to B and 20 MWh from B to A. However, since the activated quantity is unknown, reserve allocations cannot be superposed (netted) like energy allocations. If all of the quantity from A to B is activated but none of the quantity from B to A, then the resulting flow is 60 MWh from A to B. In the reverse case, a 20 MWh flow from B to A happens. In general, any value between these two extremes is possible, and the outcome is simply not known at the time when procurement happens

and transmission limits are considered.

As shown in Fig. 1, the lack of superposition leads to a situation in which a substantially smaller transfer capacity is left for other uses compared to the energy-only case. If market clearing algorithms neglect this uncertainty, then procured reserve products might be unavailable for delivery when they are actually needed to support the power system.

This study aims to provide a solution technique for reserve procurement with guaranteed deliverability in the context of a joint European energy-reserve market platform. Aside from the guarantee of deliverability, we do not deal with the issue of reserve activation herein. In essence, the separation of the procurement and activation steps is feasible due to the guarantee itself. This separation is realistic because the exact price of activation is generally not known when procurement happens, and therefore no reliable economic reasoning exists to influence the activation process. On the other hand, the separation is also practical because there are already operating independent reserve activation platforms in Europe (MARI [9] for manual and PICASSO [10] for automatic activation). Furthermore, the imbalances of different European transmission system operators (TSOs) are frequently netted in practice to resolve them without reserve activation. Our proposal can be harmonized with MARI, PICASSO and imbalance netting.

It is also worth noting that TSOs usually compensate the cost of reserve procurement using properly defined imbalance settlement mechanisms. Aside from the aspiration to reduce the associated costs, the present proposal does not affect this method of compensation.

Table 1 presents a summary about the review of relevant literature concerning cross-zonal transfer capacity allocation for energy and reserves. The majority of relevant studies ([11]-[15]) investigate unit commitment algorithms. These designs cannot provide marginal clearing prices as the potential payment of post factum compensation (uplift) is part of their operation. In addition, unit commitment models are mostly relying on technical-economic parameters and are thus not fully capable to include the strategic incentives of market participants. Furthermore, these models typically assume fixed demands and omit the

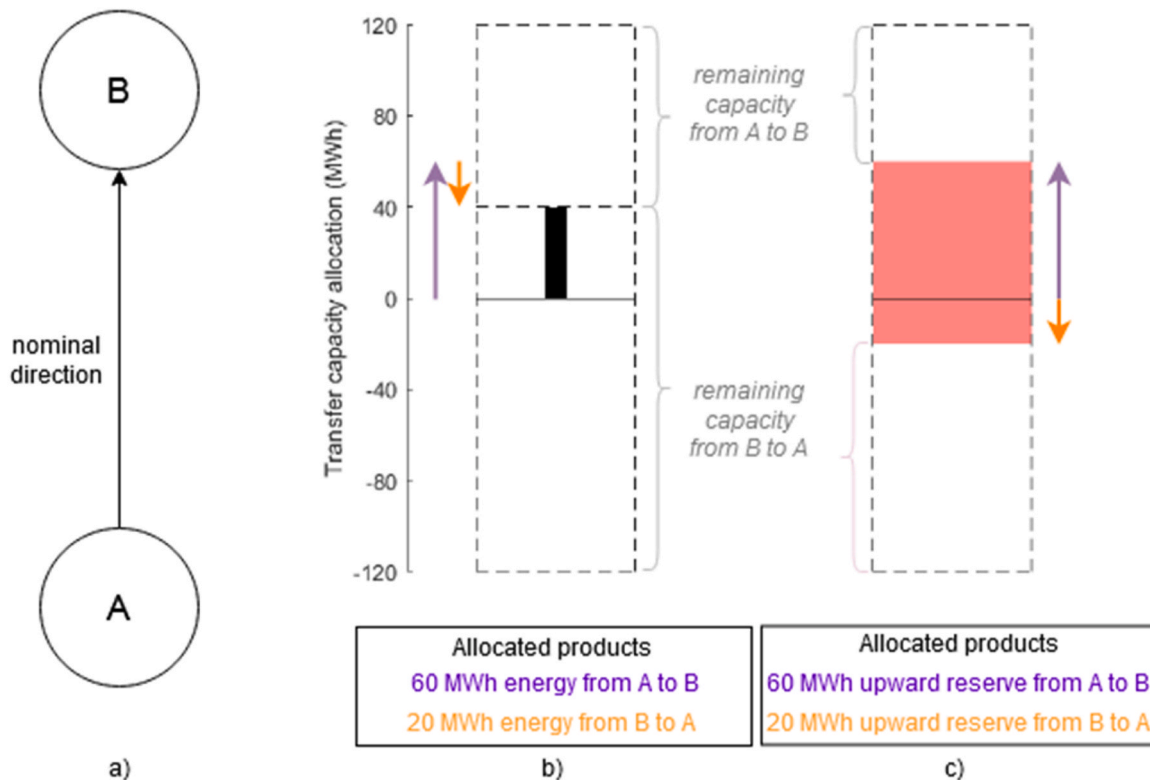


Fig. 1. Illustration of a single network line's transfer capacity allocation: a) nominal direction of the line, b) energy allocation, c) upward reserve allocation. Remaining transfer capacities are highlighted for both b) and c).

Table 1

Market design features of the public clearing algorithms dealing with the reserve deliverability issue. The present proposal combines all the advantageous features.

Source	Non-convex orders	Marginal prices for allocated bids	Energy and reserve co-allocation	Deterministic	Flow-based network model
[11]	✓			✓	
[12]	✓			✓	
[13]	✓		✓	✓	
[14]	✓		✓	✓	✓
[15]	✓		✓		✓
[16]		✓			✓
[17]		✓			✓
[18]		✓	✓		✓
This paper	✓	✓	✓	✓	✓

modeling of demand elasticity. On the other hand, the remaining proposals ([16]-[18]) assume markets without non-convex bids. The latter choice makes it possible to provide marginal allocations but the resulting designs are not realistic due to the strong non-convex properties of many generators (e.g. substantial fixed costs and minimal operating powers). European electricity markets handle non-convexities through the application of primal-dual optimization algorithms such as the pan-European clearing algorithm EUPHEMIA [19]. EUPHEMIA is capable of clearing non-convex orders while providing marginal pricing for every allocated bid. In order to provide a solution that is compatible with European market designs, our proposal provides this functionality as well.

As mentioned above, the allocation of energy and reserve product in the day-ahead timeframe might be executed either sequentially or simultaneously. Joint allocation is routinely performed by unit commitment algorithms in several parts of the world (e.g. in the US) as reflected in [13]-[15]. The simplified market in [18] follows the same approach. Nonetheless, these algorithms are not compatible with the European market where the emphasis is on self-scheduling and marginal pricing without uplift payments to manage non-convexities or revenue insufficiencies. The present proposal combines these features with energy-reserve co-allocation.

The last two columns of Table 1 examine other beneficial features. Firstly, it is advantageous from the practical viewpoint if the constructed algorithm is deterministic. Although the activation of reserves is uncertain at the time of procurement, this uncertainty can be handled in a deterministic way to provide securely working allocations. Our proposal applies robust optimization to create deterministic solutions from uncertain inputs. Stochastic algorithms such as [15]-[18] are important for research purposes but their actual application is hindered by existing routines and expectations. Secondly, the last column of Table 1 shows that our proposal applies a flow-based network model. This kind of model is more complex but it can provide more efficient exploitation of the grid compared to simpler models based on available transfer capacities (ATCs) used e.g. in [11]-[13]. Existing European markets also aim for flow-based network representation [19].

The scientific contribution of the present paper is twofold:

- Firstly, a new clearing formulation is presented for the combined trading of energy and reserves in a European context where the cross-zonal allocation of both energy and reserves is allowed. For reserve procurement, the model provides the guarantee of deliverability. It implies the solution of a Mixed Integer Linear Problem (MILP), therefore it can be considered computationally efficient.
- Secondly, realistic case studies are provided to demonstrate the operation of the proposed model. Simulation results can be used to assess computational adequacy and also to gain insights into market processes when transfer capacity is allocated for both energy and potential reserve transmission. Based on the case studies, a comparative simulation is provided to verify better economic performance relative to sequential energy-reserve clearing.

Section 2 describes the proposed solution in detail including the

equations of the constructed mathematical program. Sections 3 and 4 present the case studies and the discussion of contributions. Remaining research questions are described in Section 5 while conclusions are drawn in Section 6.

2. Proposal for deliverable cross-zonal reserves in Europe

2.1. Clearing algorithm framework

The operation of the today's power system requires three critical decisions in the day-ahead timeframe [20]:

- the allocation of energy supply to satisfy demand,
- the allocation of network transmission capacity to transport energy and equalize energy prices,
- the procurement of control reserves to maintain reliable operation in the face of potential contingencies.

As already described in the introduction, due to the interdependence of these market questions, it is more efficient to handle them in a joint, integrated design. Nonetheless, full integration is not yet achieved in practice. North American markets allocate energy and reserves on a single platform with unit commitment algorithms, but they could not overcome the difficulties of geographical integration so far i.e. a substantial part of transfer capacities are traded separately. On the other hand, European markets optimize energy and network transfer capacities in a combined way with large-scale implicit auctions, but reserves are considered separately.

The most important obstacle in the pursuit of reserve trade integration in Europe is that the task of the all-European clearing algorithm [19] is very demanding computationally, even with energy-only products. The main reason of this computational difficulty is the emphasis on uniform marginal pricing and the opportunity of self-scheduling for generators. In contrast to North American markets, individual compensation is not paid to participants after clearing, therefore uniform marginal pricing is strictly required for every allocated bid. In turn, the lack of uplift payments makes it possible to loosen regulation and let participants to schedule themselves autonomously instead of closely supervised central unit commitment. Although computationally uplift payments may be easier, there are concerns on gaming, transparency and discriminatory pricing there [21].

The European requirement of uniform marginal pricing is problematic because of the presence of non-convexities. A crucial challenge for all electricity markets is that many generators – especially thermal power plants – have strong non-convex properties such as substantial fixed costs and minimal operating loads. Markets cannot neglect these properties but their representation in the clearing algorithm is possible only with non-convex orders i.e. integer (binary) variables in the constructed optimization problems. Full marginal pricing is mathematically impossible for non-convex orders. This is why North American markets allow post-factum uplift payment for non-convex bidders. In Europe, on the other hand, marginal pricing is required for every allocated bid and deviations are restricted to happen only for refused non-convex orders, a

phenomenon called paradox rejection. In order to restrict the deviation from uniform marginal pricing i.e. to prohibit paradox acceptance, the values of allocated quantities (primal variables in the optimization) and clearing prices (dual variables) have to be calculated and constrained simultaneously. A mathematical problem with primal-dual structure is required which is inherently more complicated than the North American case where only allocations are calculated by the clearing algorithm and clearing prices are determined afterwards (along with the necessary uplifts).

There are three different approaches to construct a clearing algorithm capable of this task: they are referred to as A1, A2 and A3 herein. A1 involves a problem-specific iterative process in which different subproblems are created to find good objective values and feasible solutions. EUPHEMIA [19] follows A1 as well as the public algorithms in [22] and [23] with subtle differences in fine-tuned details. Although EUPHEMIA operates successfully for several years, it can only be categorized as a heuristic algorithm. An opportunity exists to enhance its performance by abandoning A1 i.e. by integrating its subproblems into a single standard optimization problem that is simply manageable for state-of-the-art solver routines [24]. A2 and A3 can be considered as attempts to create this standard optimization problem. The basic problem class in question is MILP for both cases.

A2 formulates primal-dual constraints (including complementarity slackness) as logical “if-then” conditions. This formulation is based on the COSMOS algorithm [25] but several additional features are available e.g. complex orders [26], unified purchase prices [24] and even combined energy-reserve orders (in simple form [5] or with complex linking conditions [8]). The logical “if-then” conditions imply the introduction of auxiliary integer variables [27].

A3 is described in detail in the PhD thesis of Mehdi Madani [28]. Its main novelty is that complementary slackness conditions are collectively enforced by the explicit coercion of strong duality as a single linear constraint. This technique eliminates auxiliary integer variables, an accomplishment that suggests enhanced computational performance compared to A2. On the other hand, the available features are not equivalent because – unlike A2 – A3 is unable to handle simple linear bids and unified purchase prices without problem-specific techniques while a public formulation of Scalable Complex Orders is available for A3 [29] but not for A2. The computational performances of A2 and A3 have been compared with an initial simple feature set [30] but the results are not decisive.

A3 has been selected as the approach to follow during the present research. The core model of A3 in the present context assumes an multi-hour market with simple step bids, block orders and a flow-based network model. The corresponding equations are listed herein.

$$\max \left\{ - \sum_e ACC_e q_e p_e - \sum_{eb} ACC_{eb} p_{eb} \sum_t q b_{eb,t} \right\} \quad (1)$$

$\forall t:$

$$- \sum_z NP_{z,t} = 0 \quad (2)$$

$\forall z, \forall t:$

$$- \sum_{\mathcal{Z}\{e\}=z, \mathcal{T}\{e\}=t} ACC_e q_e - \sum_{\mathcal{Z}\{eb\}=z} ACC_{eb} q b_{eb,t} + NP_{z,t} = 0 \quad (3)$$

$$- ECP_t + MCP_{z,t} + \sum_{\mathcal{T}\{c\}=t} ptdf_{c,z} SHF_c = 0 \quad (4)$$

$\forall e:$

$$ACC_e \leq 1 \quad (5)$$

$$- q_e MCP_{\mathcal{Z}\{e\}, \mathcal{T}\{e\}} + SP_e \geq - q_e p_e \quad (6)$$

$\forall eb:$

$$ACC_{eb} \leq 1 \quad (7)$$

$$ACC_{eb} \in \mathbb{Z} \quad (8)$$

$$ACC_{eb} > 0 \rightarrow$$

$$- \sum_t q b_{eb,t} MCP_{\mathcal{Z}\{eb\}, t} + SP_{eb} \geq - p_{eb} \sum_t q b_{eb,t} \quad (9)$$

$\forall c:$

$$\sum_z ptdf_{c,z} NP_{z, \mathcal{T}\{c\}} \leq ram_c \quad (10)$$

$$\begin{aligned} & - \sum_e ACC_e q_e p_e - \sum_{eb} ACC_{eb} p_{eb} \sum_t q b_{eb,t} \\ & \geq \sum_e SP_e + \sum_{eb} SP_{eb} + \sum_c ram_c SHF_c \end{aligned} \quad (11)$$

$$\forall ACC, \forall SP, \forall SHF \geq 0 \quad (12)$$

Aside from differences in notation, the core model (1)-(12) can be considered as a close equivalent of the model described in Chapter II of [28] with the same mathematical background, therefore we do not present its detailed derivation herein. The complete list of notations can be found in Appendix A.

The names of decision variables are written in capital letters. Indices e , eb , t , z and c refer to simple bids, block orders, trading hours, bidding zones and critical network branches with critical outages (CBCOs), respectively, (Each CBCO includes a single transmission limit of a single line or transformer in a single trading hour for a constraining network configuration.) The objective function (1) is called social welfare (SW), it equals the difference of summarized demand utility and summarized supply cost. ACC is the acceptance ratio and p is the submitted price of each bid. The submitted quantity parameter is q for simple bids and qb for multi-hour block orders. For the sake of brevity, supply quantity parameters are assumed to be positive and demand quantities to be negative. This convention makes it possible to handle each order type as a single set with identical equations.

- For demand orders, the negative quantity parameter and the negative signs in (1) lead to a positive sum of money i.e. demand utilities are added to SW.
- For supply orders, the positive quantity parameter and the negative signs in (1) lead to a negative sum of money i.e. supply costs are subtracted from the SW.

The optimization constraints (2)-(12) can be classified into three categories. The first category consists of (primal) quantity conditions, namely, (2), (3), (5), (7), (8) and (10). The summarized net position of the market is fixed to zero in (2) i.e. the total allocated supply and demand quantities must be equal. Zonal net positions (NP) are calculated in (3) where $\mathcal{Z}\{i\}$ and $\mathcal{T}\{i\}$ are the bidding zone and trading hour in which bid i is submitted. Acceptance ratios cannot exceed 1 as (5) and (7) dictate. Block orders have the non-convex fill-or-kill property, therefore their acceptance is binary (8). Flow-based transmission limits are given in (10) with power transfer distributions factor ($ptdf$) and remaining available margin (ram) parameters. The flow-based network model requires the selection of an arbitrary price zone as the hub (i.e. the nominal target of zonal exports and the nominal source of zonal imports). Every $ptdf$ value is zero for the hub by definition.

The second and third category is derived from the primal equations. The former includes (dual) price conditions (4), (6). Zonal energy clearing prices are denoted by MCP while ECP is the general energy clearing price. $\mathcal{T}\{c\}$ is the trading hour of CBCO c . Shadow prices of transmission limits and bid surpluses are calculated in SHF and SP variables. The third category of constraints (9), (11), (12) represent the connection between the primal and dual parts of the formulation. The

logical premise in (9) means that block rejection can happen regardless of prices i.e. it can be paradoxical. Meanwhile, strong duality is explicitly specified in (11): this single condition implies the satisfaction of all complementary slackness criteria. Trivial variable bounds are listed in (12).

In the context of this problem, the fulfillment of complementary slackness criteria has three important aspect. Firstly, every simple energy bid is allocated marginally according to their zonal MCP level i.e. in-the-money bids are accepted an out-of-the-money bids are rejected. Secondly, block orders are accepted only if they are not out-of-the-money considering their zonal MCPs. Thirdly, SP variables will be determined according to the following definitions:

- For a supply order, the bid surplus equals the sum of money received *in excess* of the supply cost as specified in the bids price.
- For a demand order, the bid surplus is the *reduction* of payment compared to the maximal sum of money the bidder would be willing to pay for the same allocation (i.e. the bid's utility as specified in the bid price).

The remuneration of simple bid e happens according to the following formula:

$$ACC_e q_e MCP_{\mathcal{Z}\{e\}, \mathcal{F}\{e\}} \quad (13)$$

Note that the quantity sign convention leads to a positive payment (to the bidder) for supply bids and a negative payment (from the bidder) for demand bids.

The bid surplus definition is the same for block orders. However, due to their multi-hour structure, their settlement must include all trading hours:

$$\sum_c ACC_{eb} q_{eb,t} MCP_{\mathcal{Z}\{eb\}, t} \quad (14)$$

2.2. Robust optimization of reserve procurement

The market clearing model is extended herein to handle upward and downward reserve (UR and DR) procurement with guaranteed deliverability. The first step of the extension is to introduce reserve bids.

The reserve demand for both UR and DR is specified in simple bids similarly to simple energy orders. These bids are cleared and remunerated the same way as energy demand bids, the only difference is that they have their own market prices. The result includes a single acceptance ratio variable (ACC) for each bid following marginal pricing rules.

Reserve supply bids, on the other hand, are handled differently. Although their parameters are similar to simple bids (one bid quantity and one bid price), the clearing algorithm views them separately: they are allocated for specific target zones. The difference can be most easily shown in a comparison with energy supply bids. The latter are cleared with the usual “zone-to-all” assumption i.e. accepted energy supply quantities have a source zone (where the bid is submitted) but target zones are not defined for them at any step during the clearing process. The exact network routes through which transactions take place are not specified in the clearing solution. As described in the introduction, it is sufficient in this case to deal with only netted flows without differentiating individual transactions. In contrast, reserve supply quantities are cleared with a “zone-to-zone” approach i.e. they have both source and target zones in the eventual solution because cross-zonal allocated quantities cannot be netted for reserves. Reserve supply bids have acceptance variables (called $ZACC$) for all potential target zones, and each MWh of their accepted quantity is dedicated to a single target.

Zone-to-zone clearing makes it possible to handle the uncertain flows arising from deployment events. Robust optimization as described in [31] is applied to create an adequate mathematical program for this approach. This technique that has already been proposed for several other uncertain problems in the power system such as the consideration

of security criteria in unit commitment [32], the selection of photovoltaic plant locations [33] and the scheduling of active distribution networks [34].

The effects by uncertain reserve deployment flows can be taken into account with the modification by flow-based transmission limits (5). Flow components of UR and DR must be added to the left-hand side.

$$\sum_c ptdf_{c,z} NP_{z,\mathcal{F}\{c\}} + WCFU_c + WCFD_c \leq ram_c \quad (15)$$

The deployment of reserves is uncertain, and the satisfaction of the constraint is required for every possible flow. Stochastic algorithms (e.g. in [15]) handle this issue by introducing scenarios and establishing probabilities and tolerances for failure. In contrast, robust optimization provides a deterministic solution without the need of uncertainty parameters. With network limits strictly binding, no deployment scenario is allowed to violate them. Robust optimization calculates the worst-case scenario for uncertain constraints and requires feasibility for this worst case. $WCFU$ and $WCFD$ refer to worst-case reserve flows of allocated UR and DR. Although this approach possibly leads to lower solution quality in terms of objective value, it guarantees that the constraint is always satisfied. It also eliminates the need to collect a credible and comprehensive set of inspected scenarios requiring detailed analysis and potentially impairing computational efficiency [32].

The worst-case deployment flow for allocated UR in (15) can be expressed in the terms of a maximization problem.

$$WCFU_c \geq \max \left\{ \sum_{\mathcal{F}\{us\}=\mathcal{F}\{c\}} \sum_z ptdf_{c,\mathcal{Z}\{us\} \rightarrow z} ZDEP_{us,z} q_{us} \right\} \quad (16)$$

$$\forall us, \forall z$$

$$ZDEP_{us,z} \leq ZACC_{us,z} \quad (17)$$

$$ZDEP_{us,z} \geq 0 \quad (18)$$

Index us stands for UR supply bids with $ZACC_{us,z}$ and $ZDEP_{us,z}$ as the acceptance and deployment ratios of bid us for targeted bidding zone z . For the sake of brevity, zone-to-zone $ptdf$ parameters are used in (16) that can be simply calculated from the zone-to-hub values introduced earlier:

$$ptdf_{c,\mathcal{Z}\{us\} \rightarrow z} = ptdf_{c,\mathcal{Z}\{us\}} - ptdf_{c,z} \quad (19)$$

The subtraction on the right-hand side of (19) implies that the energy in question is firstly transferred from $\mathcal{Z}\{us\}$ to the hub, and then from the hub to z . This assumption about the transfer route can be made because the network model does not consider transmission losses.

The summation of (16) determines the flow value of CBCO c resulting from the deployment of reserve supply bids. This summation takes its maximal value for the worst-case flow. As (17) and (18) specify, deployment is possible only for the quantity that is allocated (procured).

In order to utilize (16)-(18) in a MILP similar to (1)-(12), an equivalent set of linear constraints is needed. A transformation method is available for this task in [31] and (16)-(18) satisfies the necessary conditions to apply this method leading to the following results:

$$WCFU_c \geq \sum_{\mathcal{F}\{us\}=\mathcal{F}\{c\}} \sum_z WCC_{c,us,z} \quad (20)$$

$$\forall us : \mathcal{F}\{us\} = \mathcal{F}\{c\}, \forall z$$

$$WCC_{c,us,z} \geq ptdf_{c,\mathcal{Z}\{us\} \rightarrow z} ZACC_{us,z} q_{us} \quad (21)$$

$$WCC_{c,us,z} \geq 0 \quad (22)$$

$WCC_{c,us,z}$ denotes the worst-case contribution to the flow of CBCO c that can arise from the deployment of UR supply bid us to target zone z . For this specific case, the equivalent constraints are easy to interpret:

- For positive zone-to-zone $ptdfs$, the corresponding $ZDEPs$ must be equal to their maximal value i.e. to $ZACCs$. The flow contribution of these bids is correctly calculated in (21) while (22) is not binding.
- If a zone-to-zone $ptdf$ is not positive, $ZDEP$ values should be minimal (zero) with the resulting flow contribution in (22) as (21) becomes inactive.

The derivation for $WCFD$ is very similar with two principal differences:

- DR supply bids (with index ds) are considered instead of UR supply bids;
- since the deployment of DR invokes a flow in the opposite direction compared to the case of UR, $ptdf_{c,z \rightarrow \mathcal{Z}\{ds\}}$ parameters are used for flow calculation (where z is the target zone for which the bid's deployment is investigated).

The equivalent set of linear constraints can be included in a market clearing formulation similar to the core model (1)-(12). The equations and their basic explanation are presented herein while the proof of their adequacy is given in Appendix B (along the lines of [28]).

$\forall up$

$$ACC_{up} \leq 1 \quad (34)$$

$$-q_{up}UCP_{\mathcal{Z}\{up\},\mathcal{T}\{up\}} + SP_{up} \geq -q_{up}P_{up}, \quad (35)$$

$\forall dp$

$$ACC_{dp} \leq 1 \quad (36)$$

$$-q_{dp}DCP_{\mathcal{Z}\{dp\},\mathcal{T}\{dp\}} + SP_{dp} \geq -q_{dp}P_{dp} \quad (37)$$

$\forall us :$

$$\sum_z ZACC_{us,z} \leq 1 \quad (38)$$

$\forall us, \forall z :$

$$-q_{us}UCP_{z,\mathcal{T}\{us\}} + SP_{us} + q_{us} \sum_{\mathcal{T}\{c\}=\mathcal{T}\{us\}} ptdf_{c,z \rightarrow \mathcal{Z}\{us\}} SHWC_{c,us,z} \geq -q_{us}P_{us} \quad (39)$$

$$\max \left\{ -\sum_e ACC_e q_e p_e - \sum_{eb} ACC_{eb} P_{eb} \sum_t q_{b,eb,t} - \sum_{us} q_{us} P_{us} \sum_z ZACC_{us,z} - \sum_{up} ACC_{up} q_{up} P_{up} - \sum_{ds} q_{ds} P_{ds} \sum_z ZACC_{ds,z} - \sum_{dp} ACC_{dp} q_{dp} P_{dp} \right\} \quad (23)$$

$\forall t$

$$-\sum_z NP_{z,t} = 0 \quad (24)$$

$\forall z, \forall t$

$$-\sum_{\mathcal{Z}\{e\}=z, \mathcal{T}\{e\}=t} ACC_e q_e - \sum_{\mathcal{Z}\{eb\}=z} ACC_{eb} q_{b,eb,t} + NP_{z,t} = 0 \quad (25)$$

$$-ECP_t + MCP_{z,t} + \sum_{\mathcal{T}\{c\}=t} ptdf_{c,z} SHF_c = 0 \quad (26)$$

$$-\sum_{\mathcal{Z}\{up\}=z, \mathcal{T}\{up\}=t} ACC_{up} q_{up} - \sum_{\mathcal{T}\{us\}=t} ZACC_{us,z} q_{us} = 0 \quad (27)$$

$$-\sum_{\mathcal{Z}\{dp\}=z, \mathcal{T}\{dp\}=t} ACC_{dp} q_{dp} - \sum_{\mathcal{T}\{ds\}=t} ZACC_{ds,z} q_{ds} = 0 \quad (28)$$

$\forall e$

$$ACC_e \leq 1 \quad (29)$$

$$-q_e MCP_{\mathcal{Z}\{e\},\mathcal{T}\{e\}} + SP_e \geq -q_e p_e \quad (30)$$

$\forall eb$

$$ACC_{eb} \leq 1 \quad (31)$$

$$ACC_{eb} \in \mathbb{Z} \quad (32)$$

$$ACC_{eb} > 0 \rightarrow$$

$$-\sum_t q_{b,eb,t} MCP_{\mathcal{Z}\{eb\},t} + SP_{eb} \geq -P_{eb} \sum_t q_{b,eb,t} \quad (33)$$

$\forall ds$

$$\sum_z ZACC_{ds,z} \leq 1 \quad (40)$$

$\forall ds, \forall z :$

$$-q_{ds}DCP_{z,\mathcal{T}\{ds\}} + SP_{ds} + q_{ds} \sum_{\mathcal{T}\{c\}=\mathcal{T}\{ds\}} ptdf_{c,z \rightarrow \mathcal{Z}\{ds\}} SHWC_{c,ds,z} \geq -q_{ds}P_{ds} \quad (41)$$

$\forall c$

$$\sum_z ptdf_{c,z} NP_{z,\mathcal{T}\{c\}} + WCFU_c + WCFD_c \leq ram_c \quad (42)$$

$$WCFU_c \geq \sum_{\mathcal{T}\{us\}=\mathcal{T}\{c\}} \sum_z WCC_{c,us,z} \quad (43)$$

$$WCFD_c \geq \sum_{\mathcal{T}\{ds\}=\mathcal{T}\{c\}} \sum_z WCC_{c,ds,z} \quad (44)$$

$\forall c, \forall us : \mathcal{T}\{us\} = \mathcal{T}\{c\}, \forall z :$

$$ptdf_{c,z \rightarrow \mathcal{Z}\{us\}} q_{us} ZACC_{us,z} \leq WCC_{c,us,z} \quad (45)$$

$$-SHWC_{c,us,z} + SHF_c \geq 0 \quad (46)$$

$\forall c, \forall ds : \mathcal{T}\{ds\} = \mathcal{T}\{c\}, \forall z :$

$$ptdf_{c,z \rightarrow \mathcal{Z}\{ds\}} q_{ds} ZACC_{ds,z} \leq WCC_{c,ds,z} \quad (47)$$

$$-SHWC_{c,ds,z} + SHF_c \geq 0 \quad (48)$$

$$\begin{aligned}
 & - \sum_e ACC_e q_e p_e - \sum_{eb} ACC_{eb} p_{eb} \sum_i q_{b_{eb,i}} - \sum_{us} q_{us} p_{us} \sum_z ZACC_{us,z} - \sum_{up} ACC_{up} q_{up} p_{up} - \sum_{ds} q_{ds} p_{ds} \sum_z ZACC_{ds,z} - \sum_{dp} ACC_{dp} q_{dp} p_{dp} \\
 & \geq \sum_e SP_e + \sum_{eb} SP_{eb} + \sum_{us} SP_{us} + \sum_{up} SP_{up} + \sum_{ds} SP_{ds} + \sum_{dp} SP_{dp} + \sum_c ram_c SHF_c
 \end{aligned} \tag{49}$$

$$\forall ACC, \forall ZACC, \forall WCC, \forall SP, \forall SHF, \forall SHWC \geq 0 \tag{50}$$

The SW calculation (23) incorporates the utilities and costs of reserve demand and supply orders. Index *up* and *dp* stand for simple UR and DR demand bids, respectively. The bid quantity sign convention described for (1)-(12) remains in place for (23)-(50).

Primal conditions include the following categories:

- trade balance equalities for energy (24), (25), UR (27) and DR (28) that specify the equality of supply and demand allocations for the corresponding product,
- trivial conditions on acceptance ratios (29), (31), (32), (34), (35), (38), (40),
- and the robust model of flow-based congestion management (42)-(45), (47) following the scheme specified earlier in (15) and (20)-(22).

The list of dual conditions includes (26), (30), (35), (37), (39), (41),

(46) and (48), these are formulated applying standard duality theory (see Appendix B). *UCP* and *DCP* denote the hourly zonal clearing prices of UR and DR while *SHWCs* are the shadow prices arising from the restrictions on worst-case flow contributions. The primal-dual connection is specified in the conditions of block order clearing (33), strong duality (49) and non-zero variable bounds (50).

3. Case studies

3.1. The simulated scenario

The simulated market consists of five bidding zones named from A to E in the network configuration shown in Fig. 2. The highlighted values (in grey) represent the transfer capacities of corresponding lines in both directions. Arrows denote the nominal direction of each network link. Although the flow-based network model is able to consider intra-zonal network lines, the simulation includes only cross-zonal lines for the

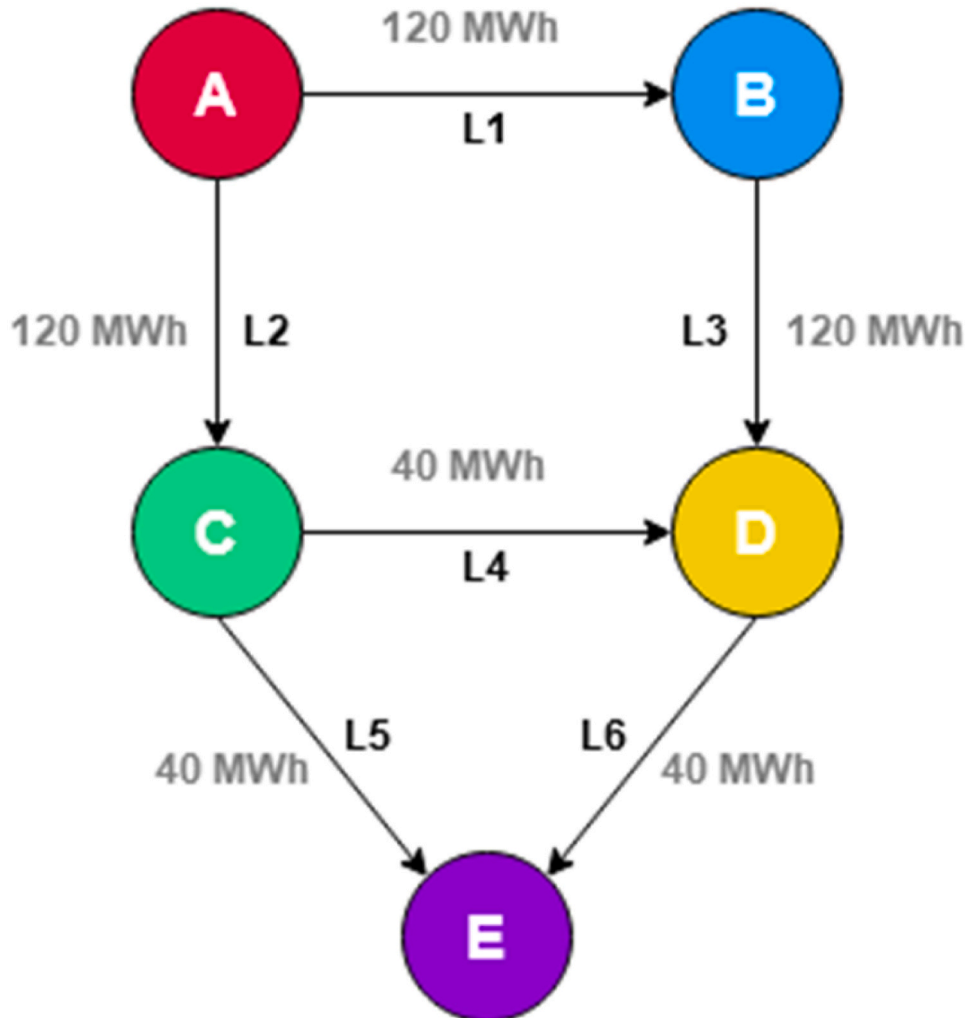


Fig. 2. Network configuration of the simulated market.

Table 2
The construction of simple energy bids for the simulated market.

Bidding zone	Data source	Modification of bid quantities (uniform distribution)	Offset of bid prices (uniform distribution)
A	individual CROPEX bids	140% to 260%	±20 EUR/MWh
B	individual OPCOM bids	140% to 260%	±20 EUR/MWh
C	individual CROPEX bids	-	-
D	individual OPCOM bids	-	-
E	individual CROPEX bids	49% to 91%	±20 EUR/MWh

sake of transparency. (It can be argued that the main bottlenecks on of the European grid are also cross-zonal.) A realistic set of zone-to-hub *ptdf* parameters have been published in [35] for the layout in Fig. 2.

$$ptdf = \begin{pmatrix} 0.27 & -0.45 & 0 & -0.18 & -0.09 \\ 0.73 & 0.45 & 0 & 0.18 & 0.09 \\ 0.27 & 0.55 & 0 & -0.18 & -0.09 \\ -0.18 & -0.36 & 0 & -0.55 & -0.27 \\ -0.09 & -0.18 & 0 & -0.27 & -0.64 \\ 0.09 & 0.18 & 0 & 0.27 & -0.36 \end{pmatrix} \quad (51)$$

The rows in (51) stand for network links in the sequence of AB, BC, BD, CD, CE and DE. Columns represent the bidding zones with C defined as the hub (hence the zeros in the third column). The same network parameters are considered for every trading hour in the simulation. Six transmission limits per trading hour is a relatively small number compared to the pan-European market clearing. However, these lines are all restricted strictly enough to be congested, and therefore – being active constraints – they are useful for the purpose of demonstration.

The simple energy orders of the five bidding zones are generated from the real market data of Romanian power exchange OPCOM [36] and Croatian market CROPEX [37] (reconstructed from aggregated bid curves). The investigated period comprises seven days from 1 August to 7 August in 2022 (named Day 1 to Day 7). Table 2 provides details about the construction process for each bidding zone.

The OPCOM dataset contains a small number of block orders as well (between two and ten on each day). These orders are added to the order book of bidding zone D along with the other original OPCOM bids. In order to make the clearing problems computationally harder, sixty additional block orders are submitted with the following parameters (every random decision is based on uniform distribution):

- random bidding zone;
- thirty supply blocks and thirty demand blocks;
- equal bid quantities for all trading hours;
- the hourly bid quantity is chosen randomly between 0.5 MWh and 15 MWh;
- the bid price is chosen randomly between 20 EUR/MWh and 100 EUR/MWh.

As Table 3 shows, the summarized transfer capacity of the network lines connected to each bidding zone is less than 1.5% of the total zonal

Table 3
The summarized transfer capacities of network lines connected to bidding zones as percentages of offered energy demand quantities.

Bidding zone	Day 1	Day 2	Day 3	Day 4	Day 5	Day 6	Day 7
A	1,49	0,96	0,80	0,85	0,68	0,80	1,25
B	0,18	0,16	0,17	0,17	0,15	0,16	0,19
C	0,34	0,31	0,33	0,33	0,30	0,32	0,37
D	0,76	0,52	0,42	0,43	0,33	0,43	0,68
E	0,83	0,57	0,48	0,48	0,36	0,45	0,71

Table 4
The construction of reserve supply bids for the simulated market (in every trading hour).

Reserve product	Bidding zone	Number of bids	Bid quantity	Bid price (uniform distribution)
Upward	A	10	20 MWh	30 ± 40 EUR/MWh
	B	10	20 MWh	60 ± 40 EUR/MWh
	E	10	20 MWh	90 ± 40 EUR/MWh
Downward	A	10	10 MWh	30 ± 40 EUR/MWh
	B	10	10 MWh	60 ± 40 EUR/MWh
	E	10	10 MWh	90 ± 40 EUR/MWh

energy demand quantity; in many cases, it is less than 0.5%. The comparably small amount of transfer capacity makes it easier to demonstrate the operation of cross-zonal capacity allocation because congestions occur frequently.

Reserve product exchange happens only in bidding zones A, B and E. (For the sake of brevity, and in order to simplify the simulation, it is assumed that reserves are procured separately in C and D.) The demand side is represented by price-taking orders i.e. with bid prices at the price cap (3000 EUR/MWh). The demand quantity is 100 MWh for UR and 50 MWh for DR in all bidding zones. Reserve supply bids are considered independently from the energy supply; they are randomly generated with the parameters listed in Table 4. The overall quantity of reserve supply is sufficient to satisfy the corresponding zonal demand in all cases (200 MWh for UR and 100 MWh for DR). On the other hand, bid prices are specified to incentivize cross-zonal procurement with bidding zone B substantially more expensive than A, and E even more expensive than B. The same parameters were used repeatedly to create reserve supply bids for all trading hours.

3.2. General results

The CPLEX solver of AMPL has been used to solve the clearing problems during the numerical simulation. The seven problems are homogenous in size, structure and complexity. All of them have around 210 thousand decision variables and a similar number of constraints. The number of integer variables is between 62 and 70 (it equals the number of block orders). As the clearing result in Table 5 shows, the outcome of these daily auctions is generally similar, too. SW is around 72 million EUR (with Day 5 as an outlier with 88 million EUR), and the optimal solution is found in fewer than ten seconds in all cases. The latter result verifies the theoretical assumptions about computational efficiency. Although further tests are certainly required to assess the practical applicability of the algorithm (with numerous different test cases and fine-tuned solver settings), the accurate and quick solution at this stage can be considered advantageous.

Table 5 also provides information about the cross-zonal trade of energy and reserves. The share of cross-zonal procurement is larger than 15% for both UR and DR on all days. In contrast, less than 3% of the allocated energy is transmitted through the network in these cases. The differences of these ratios originate from the fact that significant zonal price deviations are directly specified for reserves (see Table 4) while energy price differences mainly depend on the inherent characteristics of the OPCOM and CROPEX data (see Table 2). The large share of cross-zonal reserve procurement makes it possible to conduct a preliminary investigation about its market effects.

3.3. Detailed results for a single day

The clearing solution of Day 1 (1 August 2022) is presented herein in a more detailed manner to provide an impression about relevant market processes. Zonal clearing prices of the three traded products are illustrated in Fig. 3.

Looking at the energy (MCP) chart, two distinct categories of trading hours emerge. In the hours of the first category (from the 1st to the

Table 5
General clearing results of the simulated market.

	Day 1	Day 2	Day 3	Day 4	Day 5	Day 6	Day 7
Social welfare (million EUR)	74.029	71.235	71.057	70.672	88.239	75.044	72.542
Solution time (s)	6.53	4.02	4.66	4.98	6.44	5.41	5.78
Cross-zonal energy (%)	2.59	2.42	2.80	2.75	2.66	2.90	2.51
Cross-zonal upward reserve (%)	19.05	20.80	15.16	18.83	18.33	21.49	23.63
Cross-zonal downward reserve (%)	17.5	20.30	20.49	19.94	15.95	18.33	23.30

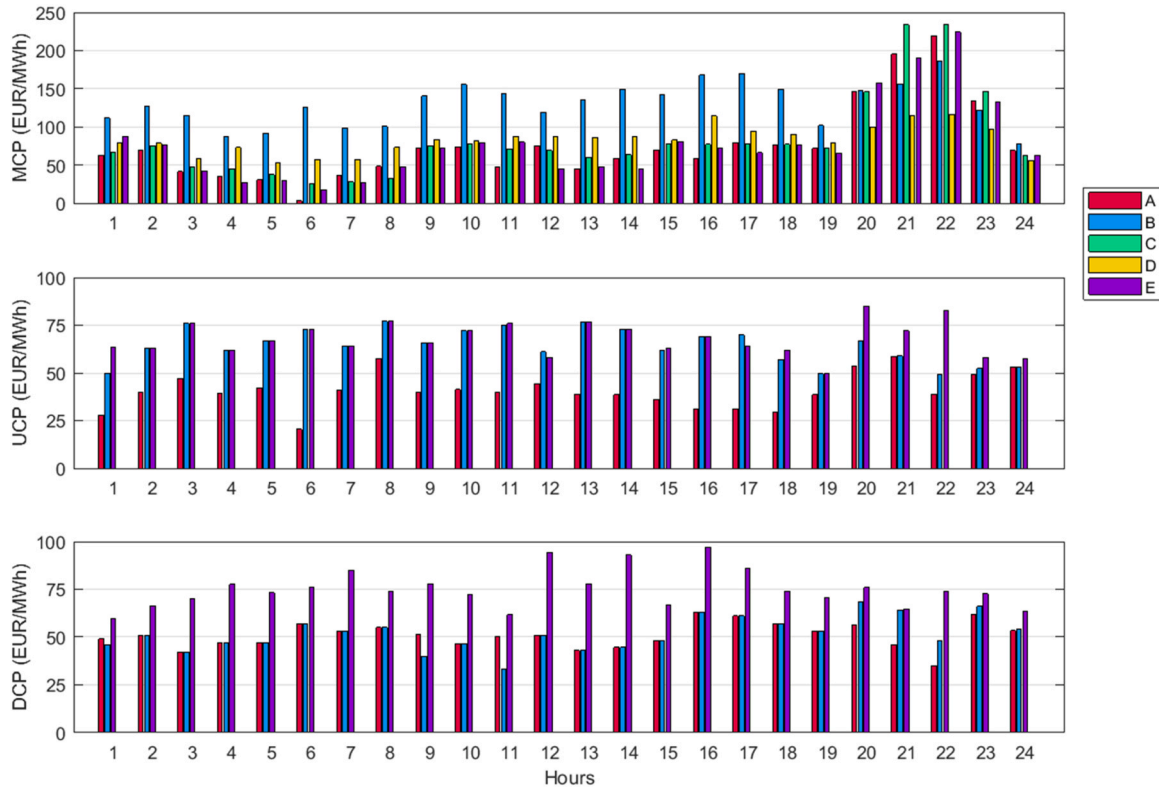


Fig. 3. Clearing prices of the simulated market (Day 1).

Table 6
Zonal net position in energy on the simulated market (Day 1).

Bidding zone	Zonal net position (MWh)	
	Hour 19	Hour 22
A	65.75	-143.0
B	-207.6	-71.38
C	56.55	55.26
D	56.60	166.7
E	28.7	-7.542

Table 7
Quantities of cross-zonal reserve procurement on the simulated market (Day 1).

Dedication	Cross-zonal reserve procurement (MWh)			
	Hour 19		Hour 22	
	Upward	Downward	Upward	Downward
A → B	0	10	20	0
A → E	60	30	40	20
B → E	20	0	0	0
B → A	0	0	0	0
E → A	0	0	0	0
E → B	0	0	0	0

19th), the energy in bidding zones B and D is generally more expensive than in the other zones. The difference arises from the fact that the simple energy bids of B and D originate from OPCOM bids while the simple energy bids of A, C and E come from CROPEX.

(see Table 2). The second category of trading hours covers the evening period (from the 20th hour to the 24th). In these hours, the price relation between OPCOM-derived and CROPEX-derived zones is changed: the energy in A, C and E is generally more expensive than in B and D.

The two reserve charts show clearing prices only in the relevant zones (A, B, E) where reserve allocation actually happens. As it is expected, reserves are generally the most expensive in bidding zone E and the cheapest in A with B in the middle (see Table 4). The two categories defined in the previous paragraph are less conspicuous but they are recognizable. In the hours from the 1st to the 19th, zonal prices are often levelled off (UCP in B and E, DCP in A and B) or even inverted in magnitude (e.g. UCP in hour 17). In contrast, the evening period has more strictly monotonous zonal prices.

Two trading hours are selected to inspect the market results of the two periods: Hour 19 and Hour 22. For these hours, the zonal net positions in energy and the quantities of cross-zonal reserve procurement are presented in Tables 6 and 7, respectively. The allocation patterns are significantly different in the two hours. It is worth noting that reserve allocations from B to A and from E to A and B are consistently zero. This is expected because SW maximization dictates that reserve in cheaper

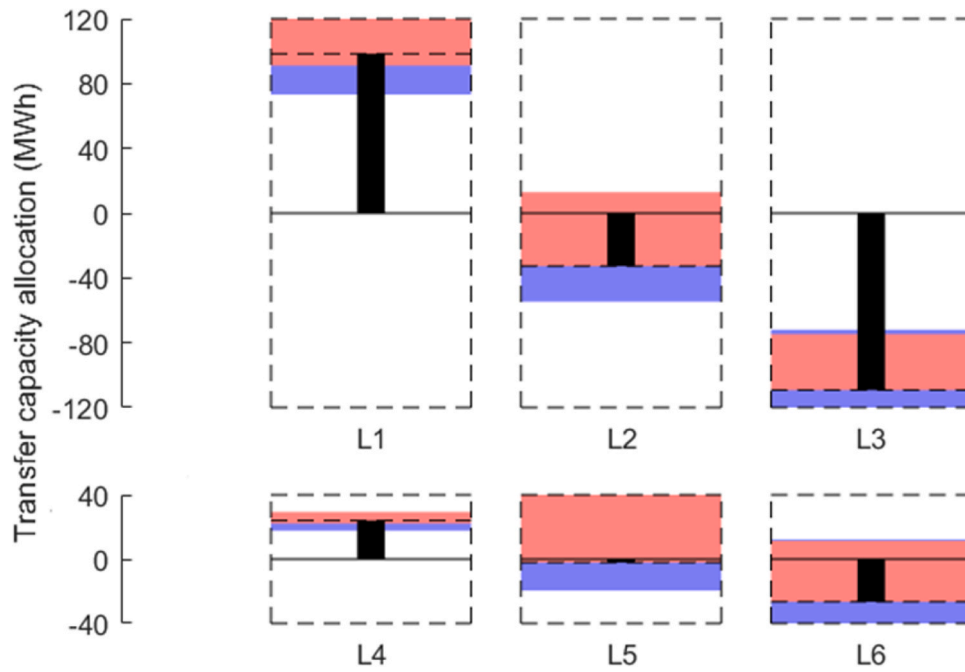


Fig. 4. Transfer capacity allocation on the simulated market (Day 1, Hour 19).

Table 8

The worst-case flow contributions of allocated cross-zonal reserve quantities on each network line of the simulated market (Day 1). The congested direction of lines is highlighted in bold.

Trading hour		Worst-case flow contributions (MWh)						
		Hour 19			Hour 22			
Product		UR		DR		UR		DR
Allocated quantity (MWh)		60	20	10	30	20	40	20
Dedication		A → E	B → E	A → B	A → E	A → B	A → E	A → E
L1	A → B	21.6	0	0	0	14.4	14.4	0
	B → A	0	7.2	7.2	10.8	0	0	7.2
L2	A → C	38.4	7.2	0	0	5.6	25.6	0
	C → A	0	0	2.8	19.2	0	0	12.8
L3	B → D	21.6	12.8	2.8	0	0	14.4	0
	D → B	0	0	0	10.8	5.6	0	7.2
L4	C → D	5.4	0	0	0	3.6	3.6	0
	D → C	0	1.8	1.8	2.7	0	0	1.8
L5	C → E	33	9.2	0	0	1.8	22	0
	E → C	0	0	0.9	16.5	0	0	11
L6	D → E	27	10.8	0.9	0	0	18	0
	E → D	0	0	0	13.5	1.8	0	9

zones must be allocated for more expensive zones and not vice versa.

Fig. 4 illustrates the transfer capacity allocation in Hour 19. Similarly to Fig. 1, black bars denote the expected energy flows arising from the energy trade i.e. the flows if no reserve is deployed. L1 and L3 transfer a substantial amount of energy to bidding zone.

B from A and D, respectively. The flows on other network links are smaller but they fit into the same picture that is also implied by the net positions shown in Table 6: B is the target of energy from all the other zones.

The transfer capacity allocated for potential reserve deployment is illustrated in Fig. 4 in red and blue for UR and DR. Firstly, it has to be noted that reserve deployment can cause flow changes in both directions depending on the product (UR or DR), the location of the supplier and the eventual target. As described in the introduction for Fig. 1, allocated transfer capacity for reserves has to be contemplated as an unavailable capacity range instead of a simple offset in directional capacities like the case of energy. The worst-case flow contributions of the cross-zonal reserve quantities are presented in Table 8 for each line in detail.

In the particular case of Hour 19, congestion happens on L1, L3, L5

and L6. Although no UR is allocated from A to B (see Table 7), L1 is congested because UR is procured in A for usage in E and the deployment of this UR creates an energy flow on L1 from A to B. In a similar way, L3 and L6 are congested because the DR allocated from A to E can invoke an energy flow from E to A, and this energy flow is a potential load on L6 from E to D and on L3 from D to B. The L5 congestion is slightly harder to explain because this line is congested in the reverse direction of its pre-deployment energy flow. Although the energy trade specifies a small amount of energy flow from E to C, the deployment of UR can reverse this flow entirely and lead to a congestion from C to E because a large amount of UR is procured from A and B to E.

The situation in Hour 22 is shown in Fig. 5 in a layout similar to Fig. 4. Bidding zones A and D have the largest import and export in this hour. Consequently, the pre-deployment flows of L1, L4 and L6 are reversed compared to Hour 19. Furthermore, the transmission from C to A on L2 is increased substantially. The cross-zonal DR procurement from A to E contributes to the congestion of L2, L3 and L4 (although the latter contribution is small compared to energy). The UR allocation from A to B also invokes potential load on L3 while L6 is saturated by the potential

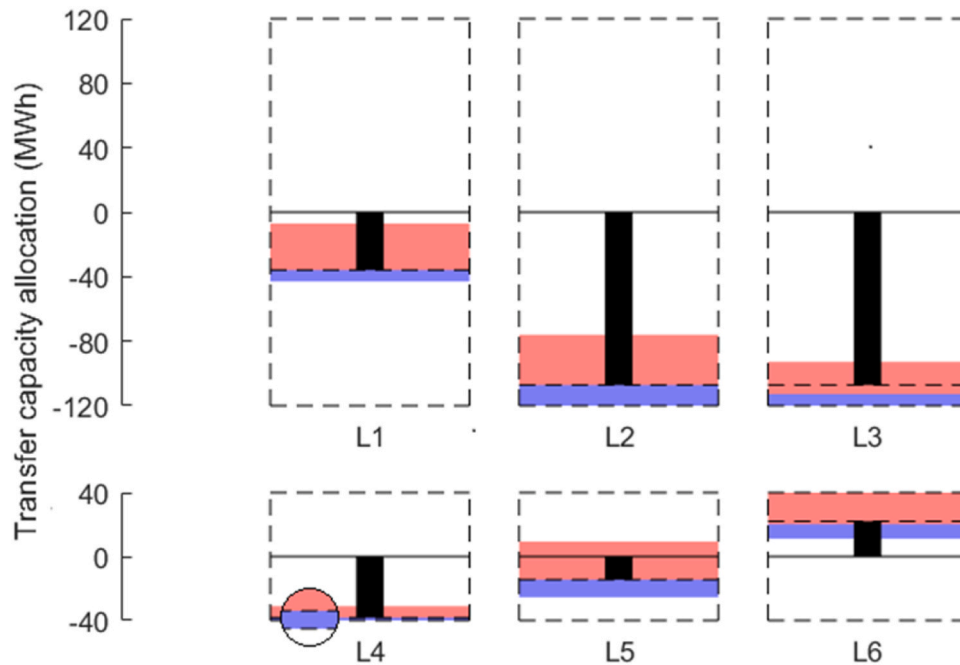


Fig. 5. Transfer capacity allocation on the simulated market (Day 1, Hour 22).

deployment of UR from A to E.

Figs. 4 and 5 both show that the capacity allocations due to reserves (the red and blue bands) on L4 are significantly smaller than on the other five network links. Network topology explains this result: L4 is not on the direct pathway between reserve-trading zones A, B and E. Although the flow-based network model distributes some of the potential reserve deployment on this indirect route, the corresponding loads are still relatively small.

The general takeaway from the investigation of Hours 19 and 22 is that the allocated energy flows have significant effects on cross-zonal reserve trading. This is the reason why reserve prices behave differently in the two cases and in the corresponding two periods of Day 1 defined earlier.

The large energy flow on L1 from A to B in Hour 19 (and in the pre-vening period) provides opportunity for DR procurement in the same direction as most of the eventual deployment would reduce the flow on this line. This DR trade leads to the equalization of DCPs in A and B. Similarly, the substantial energy flow from E to B on L6 and L3 provides an opportunity of UR export in the opposite direction leading to the levelling off of UCPs in B and E.

In Hour 22 (and in the evening period generally), reserve prices are strictly monotonous because network congestions do not allow sufficient cross-zonal procurement for price smoothing. These congestions are mostly caused by energy allocations. Between A and B, the direct route L1 is not congested but the indirect path through L2 and L3 limits reserve allocations from A to B. L2 and L3 also make it impossible for E to import large amounts of DR while the congestion of L6 restricts UR import from A and B.

3.4. Comparison to sequential allocation

In order to provide an initial assessment about the economic performance of joint energy-reserve allocation in the present context, the main results of our simulation can be compared to an equivalent case of sequential trading platforms. The sequential scenario is based on the same network and order data as the co-allocation scenario. In order to prevent the earlier energy clearing to exhaust transfer capacities completely, a fixed ratio of all transfer capacities is defined to be available only for cross-zonal reserves (and not for energy). It is called

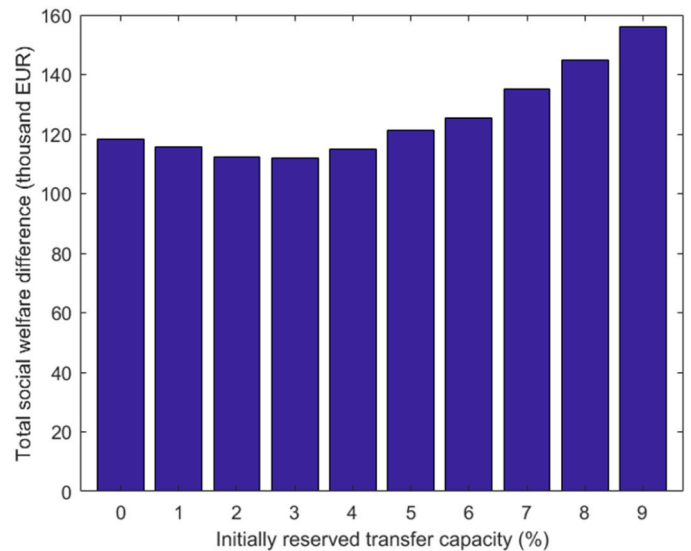


Fig. 6. Total social welfare differences between the joint and sequential allocation of transfer capacity for energy and reserves across the seven simulated trading days.

reserved transfer capacity (RTC) herein. The European Commission guideline [38] refers to this sequential approach as market-based allocation.

The clearing process consists of two steps for each day.

1. Firstly, clearing algorithm (23)-(50) is launched with all the energy orders and without any reserve orders (i.e. an energy-only market). RTC is removed from this optimization as it is unavailable for energy trade. For example, if a CBCO has an original *ram* of 200 MWh, a 5% RTC leads to a reduced *ram* of 190 MWh.
2. Secondly, clearing algorithm (23)-(50) is launched with all the reserve orders and without any energy orders (i.e. a reserve-only market). Energy flows resulting from the energy-only market are used to modify original *ram* parameters. For example, if a CBCO has

an original *ram* of 200 MWh and an energy flow of 60 MWh, then the modified *ram* is 140 MWh. (Note that energy flow can be negative if energy is transferred in an opposite, direction, and the modified *ram* is larger than 200 MWh in that case.)

The fixed RTC ratio is a critical parameter of this setup because it restricts the SW of the energy-only market without any knowledge of possible returns on the later reserve-only platform. Since the proposed co-allocation has access to implicit information about comparative SW contributions of energy and reserves, it does not require an RTC parameter at all. The total SW i.e. the sum of energy-only and reserve-only SWs is expected to be smaller than the SW of co-allocation.

As Fig. 6 illustrates, the comparative simulation has verified this assumption for the seven days of our case studies. The total SW of the sequential case is smaller the SW of the joint case regardless of the chosen RTC value. The largest total SW of the sequential variant was reached when 3% of the transfer capacity was set aside for reserves, but even in this case, joint allocation provided a better economic solution with a summarized difference of approximately 112 thousand EUR for the seven trading days.

4. Discussion

As already acknowledged in the introduction, current European electricity markets handle energy trade and reserve procurement separately (sequentially). Furthermore, reserve procurement is the responsibility of local TSOs who usually create their own platforms for this purpose with little concern about cross-zonal procurement opportunities. In essence, the market-based cross-zonal procurement without co-allocation (e.g. the mechanism presented as the sequential case in Section 3.4) is itself mostly a future step toward market integration.

Considering this context, the main contributions of this study are the concept, formulation and simulation of the proposed mathematical algorithm. It is not intended to argue for the exact implementation of the simulated market platform but rather to provide an addition to the algorithmic toolset of European market designs. To the authors' knowledge, the application of robust optimization is a novel approach to this topic. The algorithm can be adapted and refined for actual application in several ways as demonstrated e.g. by the sequential scenario in Section 3.4. Nonetheless, it is worth noting again that the joint trade of energy and reserves is beneficial not only because these products compete for the transfer capacity of the network but also because they compete for the generation capacity of power plants. Co-allocation can reach better economic outcomes compared to the separated treatment even without the consideration of cross-zonal reserve sharing [5].

The clearing formulation (23)-(50) neglects several technical and economic issues around reserve procurement because the emphasis is on cross-zonal sharing. The management of start-up costs and ramping limits presented in [8] using complex energy-reserve orders can be integrated into the model. The consideration of different reserve products – manual and automatic frequency restoration reserve (mFRR and aFRR) as well as replacement reserve (RR) – can be easily handled as well using separate trade balance equations for different products. On the other hand, hierarchical procurement e.g. the option to allocate aFRR to satisfy mFRR demand is a feature not yet formulated in this algorithmic framework.

DR demand and UR demand in neighboring zones can often (partly) eliminate each other without actual deployment as the excess electricity in the first zone can alleviate the shortage in the second one. This is the idea behind the imbalance netting process of European TSOs. As stated in the introduction, our proposal is compatible with imbalance netting. However, it must be noted that the guarantee of deliverability is valid only for activated reserves. If imbalance netting is performed to *avoid activation*, the resulting flows and the adequacy of transfer capacities still must be checked by participating TSOs.

5. Directions of further research

5.1. Consideration of the reserve deployment procedure

Robust optimization is built on the observation that all uncertain constraints are certainly feasible if they are feasible for the worst-case scenario. Accordingly, the proposed formulation (23)-(50) calculates the worst-case scenario for every CBCO i.e. the reserve deployment that invokes the largest flow in question. For this calculation, it was assumed that there is no meaningful restriction on deployment, and therefore allocated reserve quantities can be activated in any combination.

In practice, deployment decisions are complex: they have to take into account many economic and technical viewpoints. This fact is important because every restriction on deployment affects the potential worst-case scenario. In the terms of this paper, these additional conditions would appear in the UR deployment subproblem (16)-(18) and its DR counterpart: they would restrict the worst-case flows to be generally smaller than the presented model. In turn, the decision space for procurement would be larger leading to higher SW in the market clearing result.

For example, the assumption herein was that activation prices are not known in advance when reserves are procured. This is a viable assumption because these prices might be changed after procurement and also because practical deployment often considers available quantities for regulation even if they were not procured earlier. Nonetheless, activation prices are a critical factor in deployment, and their consideration might enhance the proposal. On the technical side, the question of counter-activations (simultaneous deployment of UR and DR) has similar relevance [39]. Deployment decisions might be constrained to choose only UR or only DR in a specific network area, another restriction that reduces worst-case flows. However, the definition of the areas in question is not trivial conceptually and it can be very difficult from the computational point of view. Accordingly, the appropriate algorithm to handle counter-activations is still under research.

5.2. Comparison with alternative methods

In order to investigate the performance of the proposed algorithm in detail, it should be compared to alternative methods of reserve procurement and electricity market clearing. There are several important questions for these future comparative studies.

Firstly, the algorithm presented in this paper does not provide all the market features of the pan-European power exchange clearing algorithm [19]. Missing features include simple linear bids, smart (linked or exclusive) block orders, complex orders and unified purchase prices. The addition of smart blocks is straightforward, and complex orders can also be incorporated using the descriptions available in [28]. These order types were omitted herein for the sake of brevity. On the other hand, simple linear bids and unified purchase prices pose harder questions without immediate answers. As already mentioned in Section 2.1, the primal-dual algorithm necessary for European market clearing can be implemented using another approach (A2) based on the COSMOS algorithm [25], and several missing features become available this way. A comprehensive review about the availability and necessity of different market elements might be useful to assess adequacy for practical application.

Secondly, since the computational resources and available running times for market clearing algorithms are limited, it is important to analyze the numerical performance of the proposal compared to alternative methods. The formulation as a MILP demonstrates that the proposal is on the same level of theoretical complexity as operating European clearing algorithms. The presented medium-scale case studies are promising as their solutions were quick and reliable. However, further tests and larger-scale instances are needed to analyze scalability and potential tuning options for numerical improvements. For this purpose, the ongoing FARCROSS H2020 project includes a year-long simulation of the model with real network data and orders specified

by actual market participants.

Thirdly, it might be beneficial to compare the results of robust optimization and stochastic algorithms for the same task of reserve procurement. This inspection can provide information about the inevitable economic losses that arise from the conservative consideration of worst-case scenarios. Furthermore, the investigation of totally different approaches in the literature (e.g. dynamic reserve zones) can provide ideas about further algorithm development and also about the construction of new performance metrics for cross-zonal reserve procurement.

6. Conclusion

A new market clearing algorithm is proposed for the task of cross-zonal reserve procurement. The algorithm tackles the issue of reserve activation uncertainty through the application of robust optimization. The worst-case flows resulting from deployment are calculated for all network transmission limits, and the clearing solution is coerced to be feasible for these flows.

The robust transmission limits are incorporated into a European primal-dual algorithmic framework along with non-convex block orders. The corresponding market assumes self-scheduling i.e. no unit commitment and excludes the possibility of post factum uplift payments. The clearing problem is formulated as a computationally efficient MILP with minimal number of integer variables. The viability of the proposal is demonstrated with numerical case studies based on realistic market data. The simulated clearing solutions are used to conduct a preliminary inspection of potential market effects and peculiar characteristics of cross-zonal reserve deployment in a European environment. Further tests of the proposal are conducted in the context of the ongoing FAR-CROSS H2020 project using real network parameters with bids specified

by actual market participants in the size ranges of practical applications dealing with tens of thousands of individual market bids.

There are several potential routes of further development to erase the limitations of the proposal. Firstly, it is expected to be advantageous to consider the exact deployment procedure (e.g. the effects of deployment prices and prohibited counter-activations) and secondly, the algorithm can be compared to alternative methods to assess the adequacy of its feature set, computational performance and market design quality.

Declaration of Competing Interest

The authors declare that they have no known competing financial interests or personal relationships that could have appeared to influence the work reported in this paper.

Data availability

The authors do not have permission to share data.

Acknowledgments

The authors are grateful to Beáta Polgári and Dr. Ágnes Závecz for their valuable insights regarding simulation results and Dr. István Vokony for his communicational and organizational support during the research. The contributions of Lilla Barancsik and Zoltán Jakab to the software framework of the numerical tests are highly appreciated.

The project has received funding from the European Union's Horizon 2020 research and innovation programme under grant agreement no. 864274 and from the Fund FK 137608 of the Hungarian National Research, Development and Innovation Office.

Appendix A. Nomenclature

Abbreviations.

ATC	available transfer capacity
CBCO	critical network branch with critical outage
DR	downward reserve
UR	upward reserve

Indices

c	the index of CBCOs
dp	the index of simple DR demand orders
ds	the index of DR supply orders
e	the index of simple energy bids
eb	the index of block energy orders
up	the index of simple UR demand orders
us	the index of UR supply orders
t	the index of trading hours
z	the index of bidding zones

Variables

ACC_i	the acceptance ratio of bid i
$DCP_{z,t}$	the DR clearing price of bidding zone z in trading hour t
ECP_t	the general energy clearing price in trading hour t
$MCP_{z,t}$	the energy clearing price of bidding zone z in trading hour t
$NP_{z,t}$	the net position of bidding zone z in trading hour t (in energy)
SHF_c	the shadow price of CBCO c

(continued on next page)

(continued)

$SHWC_{c,i,z}$	the shadow price arising from the restriction on worst-case flow contributions $WCC_{c,i,z}$
SP_i	the surplus of bid i
$UCP_{z,t}$	the UR clearing price of bidding zone z in trading hour t
$WCC_{c,i,z}$	the worst-case flow contribution to CBCO c of bid i deployment with target zone z
$WCFD_c$	the worst-case flow of CBCO c resulting from DR deployment
$WCFU_c$	the worst-case flow of CBCO c resulting from UR deployment
$ZACC_{i,z}$	the acceptance ratio of reserve supply bid i for target zone z
$ZDEP_{i,z}$	the deployment ratio of reserve supply bid i for target zone z

Parameters

p_i	the bid price of order i
$ptdf_{c,z}$	the zone-to-hub power transfer distribution factor of bidding zone z regarding CBCO c
$ptdf_{c,z_1 \rightarrow z_2}$	the zone-to-zone power transfer distribution from bidding zone z_1 to z_2 regarding CBCO c
q_i	the bid quantity of order i
$qb_{eb,t}$	the bid quantity of block order eb in trading hour t
ram_c	the remaining available margin of the transmission limit for CBCO c
$\mathcal{T}\{i\}$	the trading hour of market element i (order or CBCO)
$\mathcal{Z}\{i\}$	the bidding zone where order i is submitted

Appendix B. Mathematical derivation of the proposed clearing formulation

A modified version of the mathematical proof in [28] is presented herein for the proposed model (23)-(50). The derivation starts from the assumption that we know the acceptance results of block orders in advance. In this case, the primal problem is a simple linear problem. Dual variables of primal constraints are shown in brackets.

$$\max \left\{ - \sum_e ACC_e q_e p_e - \sum_{eb} ACC_{eb} p_{eb} \sum_t qb_{eb,t} - \sum_{us} q_{us} p_{us} \sum_z ZACC_{us,z} - \sum_{up} ACC_{up} q_{up} p_{up} - \sum_{ds} q_{ds} p_{ds} \sum_z ZACC_{ds,z} - \sum_{dp} ACC_{dp} q_{dp} p_{dp} \right\} \quad (B1)$$

 $\forall t :$

$$- \sum_z NP_{z,t} = 0, [ECP_t] \quad (B2)$$

 $\forall z, \forall t :$

$$- \sum_{\mathcal{Z}\{e\}=z} ACC_e q_e - \sum_{\mathcal{Z}\{eb\}=z} ACC_{eb} qb_{eb,t} + NP_{z,t} = 0, [MCP_{z,t}] \quad (B3)$$

$$- \sum_{\mathcal{Z}\{up\}=z} ACC_{up} q_{up} - \sum_{\mathcal{T}\{us\}=t} ZACC_{us,z} q_{us} = 0, [UCP_{z,t}] \quad (B4)$$

$$- \sum_{\mathcal{Z}\{dp\}=z} ACC_{dp} q_{dp} - \sum_{\mathcal{T}\{ds\}=t} ZACC_{ds,z} q_{ds} = 0, [DCP_{z,t}] \quad (B5)$$

 $\forall e :$

$$ACC_e \leq 1, [SP_e] \quad (B6)$$

 $\forall eb :$

$$ACC_{eb} \leq 1, [SP_{eb}] \quad (B7)$$

 $\forall us :$

$$\sum_z ZACC_{us,z} \leq 1, [SP_{us}] \quad (B8)$$

 $\forall up :$

$$ACC_{up} \leq 1, [SP_{up}] \quad (B9)$$

 $\forall ds :$

$$\sum_z ZACC_{ds,z} \leq 1, [SP_{ds}] \quad (B10)$$

$$\forall dp : \quad ACC_{dp} \leq 1, [SP_{dp}] \quad (B11)$$

$$\forall c : \quad \sum_z ptdf_{c,z} NP_{z,\mathcal{T}(c)} + \sum_{\mathcal{T}(us)=\mathcal{T}(c)} \sum_z WCC_{c,us,z} + \sum_{\mathcal{T}(ds)=\mathcal{T}(c)} \sum_z WCC_{c,ds,z} \leq ram_c, [SHF_c] \quad (B12)$$

$$\forall c, \forall us : \mathcal{T}(us) = \mathcal{T}(c), \forall z : \quad ptdf_{c,z \rightarrow us} q_{us} ZACC_{us,z} \leq WCC_{c,us,z}, [SHWC_{c,us,z}] \quad (B13)$$

$$\forall c, \forall ds : \mathcal{T}(ds) = \mathcal{T}(c), \forall z : \quad ptdf_{c,z \rightarrow ds} q_{ds} ZACC_{ds,z} \leq WCC_{c,ds,z}, [SHWC_{c,ds,z}] \quad (B14)$$

$$\forall ACC, \forall ZACC, \forall WCC \geq 0 \quad (B15)$$

$$\forall eba : \quad -ACC_{eba} \leq -1, [FXB_{eba}] \quad (B16)$$

$$\forall ebr : \quad ACC_{ebr} \leq 0, [FXB_{ebr}] \quad (B17)$$

The limitation of worst-case flows is unified into a single constraint (B12) and block order acceptances are fixed in (B16) and (B17). The remaining equations are explained in Section 2.2 as they are equivalent to the objective and the primal equations of (23)-(50). Indices *eba* and *ebr* denote accepted and rejected block orders.

The acceptance decisions of block orders are not known in advance. In order to handle these non-convex decisions, a bilevel optimization problem can be created with the following structure:

- The upper level looks for the optimal block acceptance decisions with the objective of maximizing SW.
- The lower level provides the best solution for any considered block acceptance configuration i.e. it calculates the solution of (B1)-(B17) for the configuration in question.

The difficulty of this approach is that bilevel optimization problems cannot be solved directly; equivalent one-level formulations must be found to handle them. The remaining part of this proof presents this equivalent formulation.

Firstly, the dual problem of (B1)-(B17) can be generated applying the duality theory of linear programming. It is another linear problem:

$$\min \left\{ \sum_e SP_e + \sum_{eb} SP_{eb} + \sum_{us} SP_{us} + \sum_{up} SP_{up} + \sum_{ds} SP_{ds} + \sum_{dp} SP_{dp} + \sum_c RAM_c SHF_c - \sum_{eba} FXB_{eba} \right\} \quad (B18)$$

$\forall z, \forall t:$

$$-ECP_t + MCP_{z,t} + \sum_{\mathcal{T}(c)=t} ptdf_{c,z} SHF_c = 0, [NP_{z,t}] \quad (B19)$$

$\forall e:$

$$-q_e MCP_{\mathcal{Z}(e),\mathcal{T}(e)} + SP_e \geq -q_e p_e, [ACC_e] \quad (B20)$$

$\forall eba:$

$$-\sum_t qb_{eba,t} MCP_{\mathcal{Z}(eba),t} + SP_{eba} - FXB_{eba} \geq -p_{eba} \sum_t qb_{eba,t}, [ACC_{eba}] \quad (B21)$$

$\forall ebr:$

$$-\sum_t qb_{ebr,t} MCP_{\mathcal{Z}(ebr),t} + SP_{ebr} + FXB_{ebr} \geq -p_{ebr} \sum_t qb_{ebr,t}, [ACC_{ebr}] \quad (B22)$$

$\forall us, \forall z:$

$$-q_{us} UCP_{z,\mathcal{T}(us)} + SP_{us} + q_{us} \sum_{\mathcal{T}(c)=\mathcal{T}(us)} ptdf_{c,z \rightarrow us} SHWC_{c,us,z} \geq -q_{us} p_{us}, [ZACC_{us,z}] \quad (B23)$$

$\forall up:$

$$-q_{up} UCP_{\mathcal{Z}(up),\mathcal{T}(up)} + SP_{up} \geq -q_{up} p_{up}, [ACC_{up}] \quad (B24)$$

$\forall ds, \forall z:$

$$-q_{ds} DCP_{z,\mathcal{T}(ds)} + SP_{ds} + q_{ds} \sum_{\mathcal{T}(c)=\mathcal{T}(ds)} ptdf_{c,z \rightarrow ds} SHWC_{c,ds,z} \geq -q_{ds} p_{ds} \quad (B25)$$

$\forall dp:$

$$-q_{dp}DCP_{\mathcal{Z}\{dp\},\mathcal{T}\{c\}} + SP_{dp} \geq -q_{dp}P_{dp}, [ACC_{dp}] \quad (B26)$$

$\forall c, \forall us : \mathcal{T}\{us\} = \mathcal{T}\{c\}, \forall z:$

$$-SHWC_{c,us,z} + SHF_c \geq 0, [WCC_{c,us,z}] \quad (B27)$$

$\forall c, \forall ds : \mathcal{T}\{ds\} = \mathcal{T}\{c\}, \forall z:$

$$-SHWC_{c,ds,z} + SHF_c \geq 0, [WCC_{c,ds,z}] \quad (B28)$$

$$\forall SP, \forall FXB, \forall SHWC, \forall SHF \geq 0 \quad (B29)$$

Secondly, the fundamental theorem of duality states that the primal (B1)-(B17) and dual (B18)-(B29) problems provide the same solution for the fixed block allocation case. Furthermore, the same solution can be described by the Karush-Kuhn-Tucker (KKT) optimality criteria:

- the satisfaction of primal conditions (B2)-(B17),
- the satisfaction of dual conditions (B19)-(B29),
- and the validity of complementary i.e. it must be true for every primal and dual condition that either the condition itself is binding or its dual variable is zero.

The complementary slackness part of the KKT criteria can be coerced by the explicit inclusion of strong duality. In other words, complementary slackness holds if the objective of the primal problem is at least as large as the objective of the dual problem.

$$\begin{aligned} & -\sum_e ACC_e q_e p_e - \sum_{eb} ACC_{eb} p_{eb} \sum_t q_{b_{eb,t}} - \sum_{us} q_{us} p_{us} \sum_z ZACC_{us,z} - \sum_{up} ACC_{up} q_{up} p_{up} - \sum_{ds} q_{ds} p_{ds} \sum_z ZACC_{ds,z} - \sum_{dp} ACC_{dp} q_{dp} p_{dp} \\ & \geq \sum_e SP_e + \sum_{eb} SP_{eb} + \sum_{us} SP_{us} + \sum_{up} SP_{up} + \sum_{ds} SP_{ds} + \sum_{dp} SP_{dp} + \sum_c ram_c SHF_c - \sum_{eba} FXB_{eb} \end{aligned} \quad (B30)$$

Thirdly, the bilevel optimization problem can be formulated in a single MILP:

- *Upper level:* The objective is to maximize SW (B1). The only upper level condition is that block acceptances are binary integers.
- *Lower level:* Primal conditions (B2)-(B17), dual conditions (B19)-(B29) and the strong duality constraint (B30) are introduced. These are all linear conditions.

A few technical modifications are needed to perform the integration of the upper and lower levels:

- We start from the problem where (B1) is the objective and (B2)-(B17), (B19)-(B29) and (B30) are the constraints.
- The actual integrality constraint (B40) of block acceptances must be included (the only upper level condition).
- Primal conditions (B16) and (B17) are removed as block acceptances are not fixed anymore.
- Instead of *FXB* variables, separate *FXBA* and *FXBR* are introduced to handle accepted and rejected block orders. As the new logical conditions (B41) and (B42) dictate, these variables can be non-zero only in the cases of block acceptance and rejection, respectively.
- Due to the separation of *FXB* variables, (B21) and (B22) can be formulated in a single Eq. (B43).

$$\max \left\{ -\sum_e ACC_e q_e p_e - \sum_{eb} ACC_{eb} p_{eb} \sum_t q_{b_{eb,t}} - \sum_{us} q_{us} p_{us} \sum_z ZACC_{us,z} - \sum_{up} ACC_{up} q_{up} p_{up} - \sum_{ds} q_{ds} p_{ds} \sum_z ZACC_{ds,z} - \sum_{dp} ACC_{dp} q_{dp} p_{dp} \right\} \quad (B31)$$

$\forall t:$

$$-\sum_z NP_{z,t} = 0, [ECP_t] \quad (B32)$$

$\forall z, \forall t:$

$$-\sum_{\mathcal{Z}\{e\}=z, \mathcal{T}\{e\}=t} ACC_e q_e - \sum_{\mathcal{Z}\{eb\}=z} ACC_{eb} q_{b_{eb,t}} + NP_{z,t} = 0, [MCP_{z,t}] \quad (B33)$$

$$-ECP_t + MCP_{z,t} + \sum_{\mathcal{T}\{c\}=t} ptdf_{c,z} SHF_c = 0, [NP_{z,t}] \quad (B34)$$

$$-\sum_{\mathcal{Z}\{up\}=z, \mathcal{T}\{up\}=t} ACC_{up} q_{up} - \sum_{\mathcal{T}\{us\}=t} ZACC_{us,z} q_{us} = 0, [UCP_{z,t}] \quad (B35)$$

$$-\sum_{\mathcal{Z}\{dp\}=z, \mathcal{T}\{dp\}=t} ACC_{dp} q_{dp} - \sum_{\mathcal{T}\{ds\}=t} ZACC_{ds,z} q_{ds} = 0, [DCP_{z,t}] \quad (B36)$$

$\forall e:$

$$ACC_e \leq 1, [SP_e] \quad (B37)$$

$$-q_e MCP_{\mathcal{Z}\{e\},\mathcal{T}\{e\}} + SP_e \geq -q_e p_e, [ACC_e] \quad (B38)$$

$\forall eb:$

$$ACC_{eb} \leq 1, [SP_{eb}] \quad (B39)$$

$$ACC_{eb} \in \mathbb{Z} \quad (B40)$$

$$ACC_{eb} < 1 \rightarrow FXBA_{eb} = 0 \quad (B41)$$

$$ACC_{eb} > 0 \rightarrow FXBR_{eb} = 0 \quad (B42)$$

$$-\sum_t qb_{eba,t} MCP_{\mathcal{Z}\{eba\},t} + SP_{eba} - FXBA_{eb} + FXBR_{eb} \geq -p_{eba} \sum_t qb_{eba,t}, [ACC_{eba}] \quad (B43)$$

$\forall us:$

$$\sum_z ZACC_{us,z} \leq 1, [SP_{us}] \quad (B44)$$

$\forall us, \forall z:$

$$-q_{us} UCP_{\mathcal{Z}\{us\},\mathcal{T}\{us\}} + SP_{us} + q_{us} \sum_{\mathcal{T}\{c\}=\mathcal{T}\{us\}} ptdf_{c,\mathcal{Z}\{us\} \rightarrow z} SHWC_{c,us,z} \geq -q_{us} p_{us}, [ZACC_{us,z}] \quad (B45)$$

$\forall up:$

$$ACC_{up} \leq 1, [SP_{up}] \quad (B46)$$

$$-q_{up} UCP_{\mathcal{Z}\{up\},\mathcal{T}\{up\}} + SP_{up} \geq -q_{up} p_{up}, [ACC_{up}] \quad (B47)$$

$\forall ds:$

$$\sum_z ZACC_{ds,z} \leq 1, [SP_{ds}] \quad (B48)$$

$\forall ds, \forall z:$

$$-q_{ds} DCP_{\mathcal{Z}\{ds\},\mathcal{T}\{ds\}} + SP_{ds} + q_{ds} \sum_{\mathcal{T}\{c\}=\mathcal{T}\{ds\}} ptdf_{c,z \rightarrow \mathcal{Z}\{us\}} SHWC_{c,ds,z} \geq -q_{ds} p_{ds} \quad (B49)$$

$\forall dp:$

$$ACC_{dp} \leq 1, [SP_{dp}] \quad (B50)$$

$$-q_{dp} DCP_{\mathcal{Z}\{dp\},\mathcal{T}\{dp\}} + SP_{dp} \geq -q_{dp} p_{dp}, [ACC_{dp}] \quad (B51)$$

$\forall c:$

$$\sum_z ptdf_{c,z} NP_{z,\mathcal{T}\{c\}} + \sum_{\mathcal{T}\{us\}=\mathcal{T}\{c\}} \sum_z WCC_{c,us,z} + \sum_{\mathcal{T}\{ds\}=\mathcal{T}\{c\}} \sum_z WCC_{c,ds,z} \leq ram_c, [SHF_c] \quad (B52)$$

$\forall c, \forall us : \mathcal{T}\{us\} = \mathcal{T}\{c\}, \forall z:$

$$ptdf_{c,\mathcal{Z}\{us\} \rightarrow z} q_{us} ZACC_{us,z} \leq WCC_{c,us,z}, [SHWC_{c,us,z}] \quad (B53)$$

$$-SHWC_{c,us,z} + SHF_c \geq 0, [WCC_{c,us,z}] \quad (B54)$$

$\forall ds : \mathcal{T}\{ds\} = \mathcal{T}\{c\}, \forall z:$

$$ptdf_{c,z \rightarrow \mathcal{Z}\{us\}} q_{ds} ZACC_{ds,z} \leq WCC_{c,ds,z}, [SHWC_{c,ds,z}] \quad (B55)$$

$$-SHWC_{c,ds,z} + SHF_c \geq 0, [WCC_{c,ds,z}] \quad (B56)$$

$$\begin{aligned} & -\sum_e ACC_e q_e p_e - \sum_{eb} ACC_{eb} p_{eb} \sum_t qb_{eb,t} - \sum_{us} q_{us} p_{us} \sum_z ZACC_{us,z} - \sum_{up} ACC_{up} q_{up} p_{up} - \sum_{ds} q_{ds} p_{ds} \sum_z ZACC_{ds,z} - \sum_{dp} ACC_{dp} q_{dp} p_{dp} \\ & \geq \sum_e SP_e + \sum_{eb} SP_{eb} + \sum_{us} SP_{us} + \sum_{up} SP_{up} + \sum_{ds} SP_{ds} + \sum_{dp} SP_{dp} + \sum_c ram_c SHF_c - \sum_{eb} FXBA_{eb} \end{aligned} \quad (B57)$$

$$\forall ACC, \forall ZACC, \forall WCC, \forall SP, \forall FXBA, \forall FXBR, \forall SHWC, \forall SHF \geq 0 \quad (B58)$$

The unified formulation (B31)-(B58) has a primal-dual structure that guarantees maximal SW for any block acceptance combination considered during the solution process. The block acceptance combination with the largest maximum is selected as the optimal solution. The only remaining task is to prohibit the paradoxical acceptance of block bids with the following formula [28]:

$\forall eb :$

$$FXBA_{eb} \leq 0 \quad (B59)$$

After the substitution of (B59) into (B31)-(B58), we get a problem that is equivalent to the proposed formulation (23)-(50).

References

- [1] Pablo González, José Villar, Cristian A. Díaz, Fco Alberto Campos, Joint energy and reserve markets: current implementations and modeling trends, *Electr. Power Syst. Res.* 109 (2014) 101–111, <https://doi.org/10.1016/j.epsr.2013.12.013>.
- [2] Milad Mousavi, Manuel Alvarez, A contract-based trading of power flexibility between a variable renewable energy producer and an electricity retailer, *Sustain. Energy Grids Netw.* 34 (2023) 101067, <https://doi.org/10.1016/j.segan.2023.101067>.
- [3] A.F. Erias, E.M. Iglesias, The daily price and income elasticity of natural gas demand in Europe, *Energy Rep.* 8 (2022) 14595–14605, <https://doi.org/10.1016/j.egyr.2022.10.404>.
- [4] Péter Kótek, Adrienn Selei, Borbála Takácsné Tóth, Balázs Felsmann, What can the EU do to address the high natural gas prices? *Energy Policy* 173 (2023) 113312 <https://doi.org/10.1016/j.enpol.2022.113312>.
- [5] D.ániel Divényi, Beáta Polgári, Ádám Sleisz, Péter Sörös, D.ávid Raisz, Algorithm design for European electricity market clearing with joint allocation of energy and control reserves, *Int. J. Electr. Power Energy Syst.* 111 (2019) 269–285, <https://doi.org/10.1016/j.ijepes.2019.04.006>.
- [6] Kenneth Van den Bergh, Erik Delarue, Energy and reserve markets: interdependency in electricity systems with a high share of renewables, *Electr. Power Syst. Res.* 189 (2020) 106537, <https://doi.org/10.1016/j.epsr.2020.106537>.
- [7] “FARCROSS Workpackages”, Online: <https://farcross.eu/workpackages/#toggle-id-8>, 27 Jun 2023.
- [8] D.ániel Divényi, Beáta Polgári, Ádám Sleisz, Péter Sörös, D.ávid Raisz, Complex energy-reserve orders for generators with income and ramping restrictions on European electricity markets, *Electr. Power Syst. Res.* 221 (2023) 109474, <https://doi.org/10.1016/j.epsr.2023.109474>.
- [9] entso-e: “Manually Activated Reserves Initiative (MARI)”. Online: https://www.entsoe.eu/network_codes/eb/mari/, 27 Oct 2023.
- [10] entso-e: “Platform for the International Coordination of Automated Frequency Restoration and Stable System Operation (PICASSO)”. Online: https://www.entsoe.eu/network_codes/eb/picasso/, 27 Oct 2023.
- [11] Kenneth Van den Bergh, Kenneth Bruninx, Erik Delarue, Cross-border reserve markets: network constraints in cross-border reserve procurement, *Energy Policy* 113 (2018) 193–205, <https://doi.org/10.1016/j.enpol.2017.10.053>.
- [12] Yonas Gebrekiros, Gerard Doorman, Stefan Jaehnert, Hossein Farahmand, Reserve procurement and transmission capacity reservation in the Northern European power market, *Int. J. Electr. Power Energy Syst.* 67 (2015) 546–559, <https://doi.org/10.1016/j.ijepes.2014.12.042>.
- [13] Maren Ihlemann, Arne van Stiphout, Kris Poncelet, Erik Delarue, Benefits of regional coordination of balancing capacity markets in future European electricity markets, *Appl. Energy* 314 (2022) 118874, <https://doi.org/10.1016/j.apenergy.2022.118874>.
- [14] Y. Chen, P. Gribik, J. Gardner, Incorporating post zonal reserve deployment transmission constraints into energy and ancillary service co-optimization, *IEEE Trans. Power Syst.* 29 (2) (2014) 537–549, <https://doi.org/10.1109/TPWRS.2013.2284791>.
- [15] F. Wang, K.W. Hedman, Dynamic reserve zones for day-ahead unit commitment with renewable resources, *IEEE Trans. Power Syst.* 30 (2) (2015) 612–620, <https://doi.org/10.1109/TPWRS.2014.2328605>.
- [16] Orcun Karaca, Stefanos Delikaraoglou, Gabriela Hug, Maryam Kamgarpour, Enabling inter-area reserve exchange through stable benefit allocation mechanisms, *Omega* 113 (2022) 102711, <https://doi.org/10.1016/j.omega.2022.102711>.
- [17] N. Viafora, S. Delikaraoglou, P. Pinson, G. Hug, J. Holbøll, Dynamic reserve and transmission capacity allocation in wind-dominated power systems, *IEEE Trans. Power Syst.* 36 (4) (2021) 3017–3028, <https://doi.org/10.1109/TPWRS.2020.3043225>.
- [18] Ruth Domínguez, Giorgia Oggioni, Yves Smeers, Reserve procurement and flexibility services in power systems with high renewable capacity: effects of integration on different market designs, *Int. J. Electr. Power Energy Syst.* 113 (2019) 1014–1034, <https://doi.org/10.1016/j.ijepes.2019.05.064>.
- [19] “EUPHEMIA Public Description. Single Price Coupling Algorithm” (2020). Online: <https://www.nordpoolgroup.com/globalassets/download-center/single-day-ahead-coupling/euphemia-public-description.pdf>, 30 Apr 2023.
- [20] Leonardo Meeus, Konrad Purchala, Ronnie Belmans, Development of the internal electricity market in Europe, *Electr. J.* 18 (2005) 25–35.
- [21] Mathieu Van Vyve: “Linear prices for non-convex electricity markets: models and algorithms” CORE Discussion Paper. Oct 2011. Online: https://dial.uclouvain.be/downloader/downloader.php?pid=boreal:91368&datastream=PDF_01, 22 Oct 2023.
- [22] Dimitris I. Chatzigiannis, Grigoris A. Dourbois, Pandelis N. Biskas, Anastasios G. Bakirtzis, European day-ahead electricity market clearing model, 2016. *Electr. Power Syst. Res.* 140 (2016) 225–239, <https://doi.org/10.1016/j.epsr.2016.06.019>.
- [23] Grigoris A. Dourbois, Pandelis N. Biskas, Dimitris I. Chatzigiannis, Novel approaches for the clearing of the European day-ahead electricity market, 2018, *IEEE Trans. Power Syst.* 33 (6) (2018) 5820–5831, <https://doi.org/10.1109/TPWRS.2018.2849645>.
- [24] Ádám Sleisz, Dr.D.ávid Raisz, Integrated mathematical model for uniform purchase prices on multi-zonal power exchanges, *Electr. Power Syst. Res.* Vol 147 (2017) 10–21.
- [25] “COSMOS description. CWE Market Coupling algorithm” Jan 2011. Online: https://hupx.hu/uploads/Piac%C3%B6sszekapcsol%C3%A1s/DAM/cosmos_algorithmus.pdf, 7 Jun 2023.
- [26] Ádám Sleisz, D.ániel Divényi, D.ávid Raisz, New formulation of power plants’ general complex orders on European electricity markets, *Electr. Power Syst. Res.* 169 (2019) 229–240, <https://doi.org/10.1016/j.epsr.2018.12.028>.
- [27] José Fortuny-Amat, Bruce McCarl, A representation and economic interpretation of a two-level programming problem, *J. Oper. Res. Soc.* 32 (9) (1981) 783–792, <https://doi.org/10.1057/jors.1981.156>.
- [28] M. Madani, “Revisiting European day-ahead electricity market auctions: MIP models and algorithms,” Ph.D. dissertation, Université catholique de Louvain, 2017.
- [29] Mehdi Madani, Mathieu Van Vyve, Revisiting minimum profit conditions in uniform price day-ahead electricity auctions, *Eur. J. Oper. Res.* 266 (3) (2018) 1072–1085.
- [30] Á. Sleisz, D. Divényi, P. Sörös, D. Raisz, Performance comparison of integrated formulations for european electricity market clearing, Ljubljana, Slovenia, 2022, 18th Int. Conf. Eur. Energy Mark. (EEM) (2022) 1–6, <https://doi.org/10.1109/EEM54602.2022.9921009>.
- [31] Bram L. Gorissen, Ihsan Yanikoğlu, Dick den Hertog, A practical guide to robust optimization, *Omega* 53 (2015) 124–137, <https://doi.org/10.1016/j.omega.2014.12.006>.
- [32] A. Street, F. Oliveira, J.M. Arroyo, Contingency-constrained unit commitment with n–K security criterion: a robust optimization approach, *IEEE Trans. Power Syst.* 26 (3) (2011) 1581–1590, <https://doi.org/10.1109/TPWRS.2010.2087367>.
- [33] Hani Gilani, Hadi Sahebi, Mir Saman Pishvae, A data-driven robust optimization model for integrated network design solar photovoltaic to micro grid, *Sustain. Energy Grids Netw.* 31 (2022) 100714, <https://doi.org/10.1016/j.segan.2022.100714>.
- [34] Ali Mehrbakhsh, Shahram Javadi, Mahmood Hosseini Aliabadi, Hamid Radmanesh, A robust optimization framework for scheduling of active distribution networks considering DER units and demand response program, *Sustain. Energy Grids Netw.* 31 (2022) 100708, <https://doi.org/10.1016/j.segan.2022.100708>.
- [35] Kenneth Van den Bergh, Erik Delarue, William D’haeseleer, “DC power flow in unit commitment models.” May 2014. Online: https://www.mech.kuleuven.be/en/tme/research/energy_environment/Pdf/wpen2014-12.pdf, 16 Jun 2023.
- [36] OPCOM, “Tranzacții – Rezultate: Informații Ordin ANRE nr.7/08.02.2017”, Online: <https://www.opcom.ro/rapoarte-pzu-curve-agregate/ro>, 25 Jun 2023.
- [37] CROPEX, “Market Data: Day-Ahead Market: Price Curves”, Online: <https://www.cropep.hr/en/market-data/day-ahead-market/price-curves.html>, 25 Jun 2023.
- [38] “Commission regulation (EU) 2017/2195 of 23 November 2017 establishing a guideline on electricity balancing. Title IV: Cross-zonal capacity for balancing services.” Online: <https://eur-lex.europa.eu/legal-content/EN/TXT/HTML/?uri=CELEX:32017R2195#d1e3830-6-1>, 27 Oct 2023.
- [39] MARI : Algorithm Design Principles.” Nov 2018. Online: https://eepublicdownloads.blob.core.windows.net/public-cdn-container/clean-documents/Network%20codes%20documents/Implementation/MARI/181102_MARI_algorithmDesignPrinciples_N-SIDE_Report_Final.pdf, 22 Jun 2023.